IS IT ME OR THE TRAIN MOVING? HUMANS RESOLVE SENSORY CONFLICTS WITH A NONLINEAR FEEDBACK MECHANISM IN BALANCE CONTROL

A PREPRINT

Lorenz Assländer
Human Performance Research Centre
University of Konstanz, Konstanz, Germany
lorenz.asslaender@uni-konstanz.de

Matthias Albrecht
Human Performance Research Centre
University of Konstanz, Konstanz, Germany
matthias.albrecht@uni-konstanz.de

Markus Gruber
Human Performance Research Centre
University of Konstanz, Konstanz, Germany
m.gruber@uni-konstanz.de

Robert J. Peterka
[1]National Center for Rehabilitative Auditory Research
VA Portland Health Care System, Portland, Oregon, USA
[2]Department of Neurology
Oregon Health & Science University, Portland, Oregon, USA
peterkar@ohsu.edu

November 14, 2024

ABSTRACT

Humans use multiple sensory systems to estimate body orientation in space. A predominant concept for the underlying multisensory integration (MSI) is the linear summation of weighted inputs from individual sensory systems. The sensory contributions change depending on context and environmental conditions. These changes are typically attributed to 'reweighting' by some higher order mechanism. We provide evidence for a conceptually different mechanism that 1) performs a multisensory correction if the reference of a sensory input moves in space and is therefore unreliable and 2) combines the corrected sensory inputs with fixed weights. The correction is based on a sensory reconstruction of the sensory reference frame motion (RFM) and allows humans to automatically counteract erroneous inputs, e.g., when looking at a moving train. The proposed RFM estimator contains a nonlinear deadzone that blocks corrections at slow velocities. We first demonstrate that this mechanism accounts for the apparent changes in sensory contributions. Secondly, we hypothesized that such a nonlinearity would distort balance responses to perturbations in a very specific way. We predicted such distortions in body sway using a balance control model. Experiments using visual scene movements confirmed the predictions. The findings indicate that the central nervous system resolves sensory conflicts by an internal reconstruction of the cause of the conflict. Thus, the mechanism links the concept of causal inference to shifts in sensory contributions, providing a cohesive picture of MSI for the estimation of body orientation in space.

Keywords multisensory integration · posture control · vision · proprioception · vestibular

1 Introduction

We experience the world through a variety of sensory inputs. It is widely understood that the central nervous system (CNS) combines these inputs to create an internal representation of the world (Imamizu et al., 2000; Laurens and Angelaki, 2017; Wolpert et al., 1995). To avoid ambiguity in this internal representation, the CNS must resolve conflicts between individual sensory inputs. This process is called 'causal inference' whereby changes in the external world are inferred from a given set of sensory inputs (Körding et al., 2007). Conflicting sensory inputs are a challenge for

MSI in human balance control. For example, visual cues contribute to balance control. However, visual cues do not always accurately encode orientation in space. Consider standing next to a train leaving the station. In this situation, relying on vision for balance control would lead us to misinterpret the moving train as self-motion. The resulting balance corrections would induce movement with the train and lead to a fall. However, normally we do not fall. This reflects the ability of the central nervous system to modulate the contribution of visual cues used to estimate our body orientation in space and maintain balance (Horak and Macpherson, 1996; Lee and Lishman, 1975). Crucially, this selective integration involves a continuous adjustment of sensory contributions depending on context and availability—a process often attributed to sensory reweighting (Nashner and Berthoz, 1978; Peterka, 2002).

To conceptually understand the underlying MSI processes, sensory inputs can be simplified as signals encoding body orientation with respect to sensory reference frames. In free stance, the reference frames are the support surface, the visual scene, and gravito-inertial space (Peterka, 2002). Creating conflicts between inputs is a classic experimental paradigm used in MSI studies. As in the example with the moving train, sensory conflicts are also ecologically relevant, as they occur in everyday life. Experimentally, RFM paradigms have been used extensively to study balance control (Pasma et al., 2015; Peterka, 2002; Kiemel et al., 2008), perception (Fetsch et al., 2009, 2012; Riecke et al., 2023) and navigation (Noel and Angelaki, 2022). These studies have shown that MSI can be represented as a weighted linear sum of individual sensory inputs. Consistent with this, CNS recordings have demonstrated that firing rates of multisensory neurons matched a weighted linear sum of their inputs (Cullen, 2019; Fetsch et al., 2012). However, as in the moving train example, context-dependent reweighting implies an underlying nonlinear processing of sensory information (Fetsch et al., 2012; Morgan et al., 2008; Peterka, 2002). The question of how sensory weights are determined, or more generally, how sensory contributions are dynamically adjusted is therefore of great importance in MSI research.

The popular framework of optimal estimation suggests that minimizing variability in the estimate is the overarching criterion for choosing weights (Dokka et al., 2010; van der Kooij and Peterka, 2011; van der Kooij et al., 2001; Morgan et al., 2008; Noel and Angelaki, 2022; Carver et al., 2006). However, this criterion itself does not explain how the central nervous system achieves reweighting (Angelaki et al., 2009). In forced choice tasks, such as estimating the size of an object (Ernst and Banks, 2002), it is reasonable to assume that probabilistic properties can be assessed over a longer time frame. However, reweighting must occur rapidly in closed-loop processes (Noel et al., 2023) when the accuracy of a source changes suddenly, e.g., when a reference frame starts to move. How the CNS achieves reweighting under such conditions is not yet fully understood.

In this study, we provide evidence for an MSI mechanism that does not rely on dynamic adjustments of sensory weights. Rather, changes in sensory contributions emerge from a nonlinear multisensory RFM estimator. As RFM is the cause of a sensory conflict, an RFM estimator is a specific implementation of the principle of causal inference in a closed loop system. The mechanism was inspired by previous studies that were able to explain nonlinear behavior typically attributed to reweighting in the perception of head and trunk rotation (Mergner et al., 1991), balance control during support surface tilts (Assländer et al., 2015; Mergner et al., 2003), and when lightly touching a moving reference with a finger (Assländer et al., 2018). However, there is still a lack of evidence for the existence of a specific mechanism that implements causal inference in closed-loop control systems.

We formulated a balance control model that included an RFM estimator for the specific case of visual scene movements. Crucially, the RFM estimator contains a nonlinear element. We rationalized that this nonlinearity must lead to specific, experimentally testable nonlinear distortions in the sway responses evoked by visual scene movements. In the present work we identified and experimentally confirmed such distortions. Our study therefore provides evidence that the central nervous system uses a nonlinear, causal RFM reconstruction to estimate body orientation in space. We also show that the mechanism is the origin of changes in sensory contributions typically attributed to sensory reweighting.

2 Results

Model description

Figure 1a represents a closed loop balance control model when viewing a moving visual scene (Figure 1b). In such a situation, the central nervous system receives sensory cues from two reference frames: One sensory input encodes body orientation relative to gravito-inertial space, φ_{space}, derived from vestibular and proprioceptive cues. The second sensory input encodes body orientation relative to the visual scene, φ_{vis}. Additionally, the rate of change (velocity) of these two inputs, $\dot{\varphi}_{space}$ and $\dot{\varphi}_{vis}$, are also available. The multisensory integration mechanism (Figure 1c) combines these signals to estimate body orientation in space, $\widehat{\varphi}_{body}$, which is used to generate torque to maintain balance. However, moving the visual scene generates a conflict between the two inputs that the CNS needs to resolve to avoid falls.

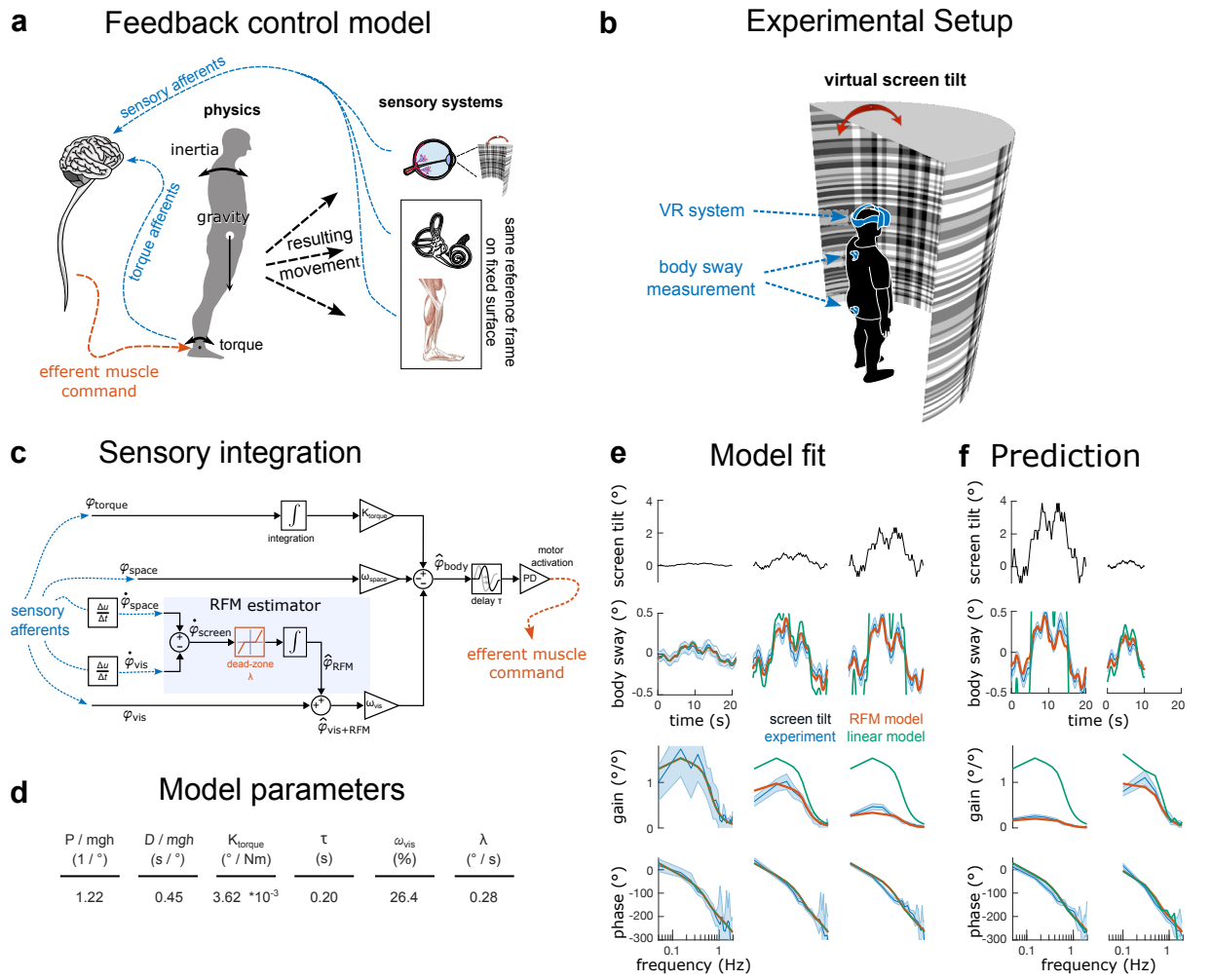

Figure 1: Conceptual balance control model and MSI mechanism, experimental setup, model fits and model predictions. a) Conceptual balance control model. Sensory inputs encoding body orientation relative to the visual scene and relative to space, as well as ankle torque. CNS integrates sensory information and generates ankle torque, correcting deviations from the desired upright position. Corrective ankle torque accelerates the body, thereby modulating the sensory inputs, making it a closed loop system. b) Experimental setup. Subjects wore a virtual reality head-mounted display and body sway was recorded from VR markers attached to hip and shoulder. Body center of mass sway, derived from hip and shoulder motion, was the primary outcome measure. Subjects stood on a fixed and level surface and viewed a richly patterned screen in the virtual environment which tilted forward and backward around the ankle joints following predefined waveforms. The setup generates balance behavior equivalent to real-world experiments (Assländer et al., 2023). c) Multisensory integration mechanism. d) Model parameters estimated from experimental data: proportional (P) and derivative (D) motor activation-gains, positive torque feedback gain (K_{torque}), time delay (τ), the visual weight (ω_{vis}), and the dead-zone velocity threshold (λ). The space-reference feedback weight was derived using the convention $\omega_{vis} + \omega_{space} = 1$. Inverted pendulum parameters (mass, center of mass height and moment of inertia) were estimated from anthropometric measures of subjects. e) Visual scene tilt waveform used for experimental sway, model sway predictions, and model fits. Experimental body sway averages across 14 cycle repetitions x 24 subjects for each amplitude (blue) are shown with shaded 95% bootstrap confidence bounds (Zoubir and Boashash, 1998). Sway responses from the nonlinear model shown in c (orange) and from a linear model for comparison (green). The linear model was identical to the model in c except that the RFM estimator was removed. f) Prediction of sway responses. The model and estimated parameters were subsequently used to predict sway responses to stimuli that were not used for parameter fits (orange) with the experimental sway responses (blue) and linear model (green) for comparison.

To this end, we propose that one component of the MSI mechanism is an RFM estimator. The idea was derived from observations in perception and earlier studies from our laboratory. Using pilot data and extensive simulations, we derived the formulation in Figure 1c as the simplest model formulation to implement this idea and to generate testable hypotheses. The model builds on an established model (Peterka, 2002), to which we added the RFM estimator to account for nonlinear behavior. Within the RFM estimator, the CNS derives a signal representing the visual scene velocity in space from the two velocity inputs: $\dot{\varphi}_{screen} = \dot{\varphi}_{space} - \dot{\varphi}_{vis}$. The RFM estimator processes $\dot{\varphi}_{screen}$ using a nonlinear dead-zone that blocks slow RFM velocities $|\dot{\varphi}_{screen}| < \lambda$ and a subsequent mathematical integration to derive the RFM estimate $\widehat{\varphi}_{RFM}$. Note that $\dot{\varphi}_{screen}$ is a velocity signal, as only a velocity dead-zone in this multisensory pathway is able to account for experimental data (see below). Then $\widehat{\varphi}_{RFM}$ is combined with φ_{vis} to form a corrected visual contribution $\widehat{\varphi}_{vis+RFM}$. In plain words, we propose that humans use visual orientation with respect to the visual scene that is corrected by the nonlinear estimate of the visual scene movement.

A second component of the MSI mechanism forms a weighted linear sum of the corrected visual contribution $\widehat{\varphi}_{vis+RFM}$ and φ_{space} with fixed weights ω_{vis} and ω_{space} using the convention $\omega_{vis} + \omega_{space} = 1$.

A third component of the MSI mechanism processes a sensory-derived measure of ankle torque φ_{torque}. The ankle torque measure is mathematically integrated and scaled (K_{torque}) before being combined with other sensory derived orientation information. The torque feedback is organized in a positive feedback configuration that generates a slowly acting component of ankle torque that moves the body toward an upright orientation. The torque feedback accounts for low-frequency behavior and might be considered as a self-calibration mechanism, i.e., it slowly corrects for potential errors of the dynamic feedback components (Missen et al., 2023). The torque feedback component is linear and therefore does not contribute to nonlinear changes in sensory contributions.

Considering the overall function of the MSI mechanism, a change in sensory contributions emerges when the visual scene velocity $\dot{\varphi}_{screen}$ exceeds the velocity threshold $\pm\lambda$ of the dead-zone. Consider a simple scenario where $\dot{\varphi}_{screen}$ is very small ($|\dot{\varphi}_{screen}| < \lambda$). In this situation $\widehat{\varphi}_{RFM}$ is zero and the MSI mechanism is a weighted linear sum with fixed weights. When $\dot{\varphi}_{screen}$ becomes larger ($|\dot{\varphi}_{screen}| > \lambda$), the dead-zone output is non-zero and its mathematical integral yields the RFM estimate $\widehat{\varphi}_{RFM}$, a distorted version of φ_{screen}. Adding $\widehat{\varphi}_{RFM}$ to the visual input φ_{vis} effectively subtracts a nonlinearly distorted version of $\dot{\varphi}_{vis}$ from φ_{vis} and adds a distorted version of $\dot{\varphi}_{space}$, whenever the RFM estimate exceeds the velocity threshold $\pm\lambda$. In terms of causal inference, the signal component exceeding λ is attributed to RFM motion by the mechanism, rather than self-motion. Thus, in this MSI mechanism, a change in sensory contributions is caused by the nonlinear RFM architecture, rather than by explicitly changing sensory weighting factors.

How much φ_{vis} is corrected depends on how much $\dot{\varphi}_{screen}$ exceeds $\pm\lambda$. The system will correct in proportion to the supra-threshold component of $\dot{\varphi}_{screen}$. When the correction becomes very large ($|\dot{\varphi}_{screen}| >> \lambda$), it leads to a saturation in sway responses. The reason is that $\widehat{\varphi}_{RFM}$ now strongly contributes, mostly canceling the visual contribution. Such saturations have been observed in several MSI studies (Mergner et al., 1991; Nashner and Berthoz, 1978; Ohshiro et al., 2011; Peterka, 2002).

Explanatory and predictive power of the model

In a first step, we tested the ability of our model to account for sway responses across different stimulus amplitudes. Twenty-four subjects viewed a moving visual scene in a virtual environment and their body sway was recorded (Figure 1b). We recorded sway responses to three pseudorandom stimuli that were identical in shape but differed in amplitude (Figure 1e, row 1). Sway responses to this amplitude series showed the expected (Assländer et al., 2023; Peterka, 2002) less than proportional increase in sway responses compared to the increase in stimulus amplitudes (Figure 1e, row 2). This behavior is a major nonlinear characteristic of human balance typically accounted for by sensory reweighting. The less than proportional increase was also reflected in the frequency response functions (FRFs), which we used to characterize stimulus/response behavior in the frequency domain. The gain (sway response to stimulus amplitude ratio; Figure 1e, row 3), greatly decreased with increasing stimulus amplitudes, whereas the phase (relative timing of stimulus and response) was similar across stimulus conditions (Figure 1e, row 4).

We used an optimization procedure to fit 6 parameters of our balance control model to these three experimental FRFs (Figure 1d). Notably, we fit one set of parameters for all three conditions simultaneously and parameters, including the weights ω_{vis} and ω_{space}, did not change across conditions. In other words, the model does not include any form of explicit sensory reweighting and all parameters reflect fixed properties of the MSI mechanism for balance control. The model accounted for the experimental FRF shapes at all three stimulus amplitudes and reproduced time-domain sway responses with a variance accounted for (VAF) of 89%, 82% and 95%, respectively (Figure 1e, row 1). For comparison, the behavior of a linear model with fixed weights and without any form of reweighting is shown in green (Figure 1e). The FRFs of the linear model do not change across conditions, reflecting the linear increase of sway amplitudes with stimulus amplitudes, leading to sway responses largely exceeding the experimental and RFM model results at

larger stimulus amplitudes. As the RFM model reproduced the under-proportional change in sway response amplitudes, the result demonstrates the ability of the model to reproduce behavior typically attributed to reweighting of sensory contributions.

Our model parameters (Figure 1d) provide interpretable quantities describing the sensory integration behavior. The visual contribution was estimated as ω_{vis} = 26.7%, resulting in ω_{space} = 73.3%. These fixed weights can be interpreted as the sensory contributions to balance during unperturbed stance when sway velocities are low and remain below the nonlinear threshold. The nonlinear dead-zone has a velocity threshold of $\lambda = \pm 0.28$ °/s, outside of which the RFM estimate starts to correct the visual contribution. The torque feedback gain (K_{torque}), feedback delay (τ) as well as motor activation stiffness and damping parameters P and D (Figure 1d) were fully in line with estimates from previous studies (Assländer et al., 2015; Peterka, 2002).

In a second step, we used the previously identified model parameters to predict sway responses to two additional pseudorandom visual stimuli that were not used in the original parameter identification procedure (Figure 1f, row 1). One stimulus had the same cycle duration as the three used for parameter identification but had a larger amplitude. The second stimulus had a smaller amplitude and its cycle duration was half that of the first three stimuli. Experimental results were in excellent agreement with RFM model predictions, in the frequency domain (Figure 1f, rows 3 and 4), as well as in the time domain with VAFs of 91% and 81%, respectively (Figure 1f, row 2).

Distortions in sway responses to sinusoidal stimuli

The ability to explain and predict responses to different stimulus amplitudes constitutes considerable evidence for the validity of the proposed MSI mechanism. We now searched for nonlinear distortions in simulated sway responses. The distortions are expected in stimuli with varying velocities, as the dead-zone blocks the RFM estimate at slow velocities, but contributes at faster velocities. Therefore, the feedback changes nonlinearly within one stimulus cycle.

As sine waves continuously change velocities, we rationalized that balance responses will show some form of nonlinear distortion. To maximize the effect, we created a waxing and waning stimulus pattern by superimposing two closely adjacent sinusoidal frequencies (Figure 2a). Using the model parameters derived from responses to the pseudorandom stimuli (Figure 1d), the model simulations predicted sway responses at the two stimulus frequencies (black arrows in Figure 2b), as would be expected in any linear model (green dots in Figure 2b). However, the model also predicted non-zero sway responses at a number of specific frequencies other than those of the stimulus (Figure 2b; red circles with values greater than zero). The experimental results were largely consistent with the predicted sway responses with spectral peaks from the experimental data occurring at the same frequencies as the model-predicted spectral peaks (Figure 2b). In the time domain, sway responses followed the predicted shape with slightly smaller experimental sway responses as predicted and a VAF of 81%. Furthermore, the experimental spectrum exhibited variable low frequency components that declined gradually with increasing frequency, aligning with spectral patterns observed during quiet stance (Laboissière et al., 2015).

We also tested whether sway responses would be distorted when using a single sine stimulus (Figure 2c). The dead-zone would again block the RFM estimate, during slow phases of the sine, thereby distorting the feedback. The predicted distortion was surprisingly small, but visible in the spectrum at 0.6 Hz (Figure 2d). In agreement with this prediction, the experimental spectrum also showed a frequency peak at 0.6 Hz. In addition, experiments showed a second small peak at 0.4 Hz, which was not predicted by the model and could be related to the simplifications used in our approach (see Discussion). Overall, the time domain sway response to the sinusoidal stimulus was predicted with a VAF of 86%.

Power-law velocity dependence

Two earlier studies (Peterka and Benolken, 1995; Mergner et al., 2005) that characterized sway responses evoked by sinusoidal visual stimuli over a range of frequencies and amplitudes provided data sets for comparison to predictions of the RFM model. Additionally, a subset of these data from 0.2 Hz tests with stimulus velocities ranging from about 0.25 to 12.5°/s were shown to be consistent with the predictions of a Bayesian inference mechanism (Dokka et al., 2010). Specifically, when various assumptions were made that were necessary for the Bayesian analysis, the analysis reproduced a power-law relationship between response gain (ratio of sway velocity to stimulus velocity) and peak visual stimulus velocity. Since Bayesian inference is widely considered to be an organizing principle in sensorimotor processing and control, we considered it relevant to determine the extent to which the RFM model reproduces this power-law relationship.

Response gain versus peak visual stimulus velocity data from the earlier studies showed approximate linear variation for 0.2 Hz stimulus frequencies when plotted on log-log axes, as expected for power-law behavior (Dokka et al., 2010). Similar power law behavior was exhibited also for data from 0.05, 0.1, and 0.4 Hz stimulus frequencies (not shown in

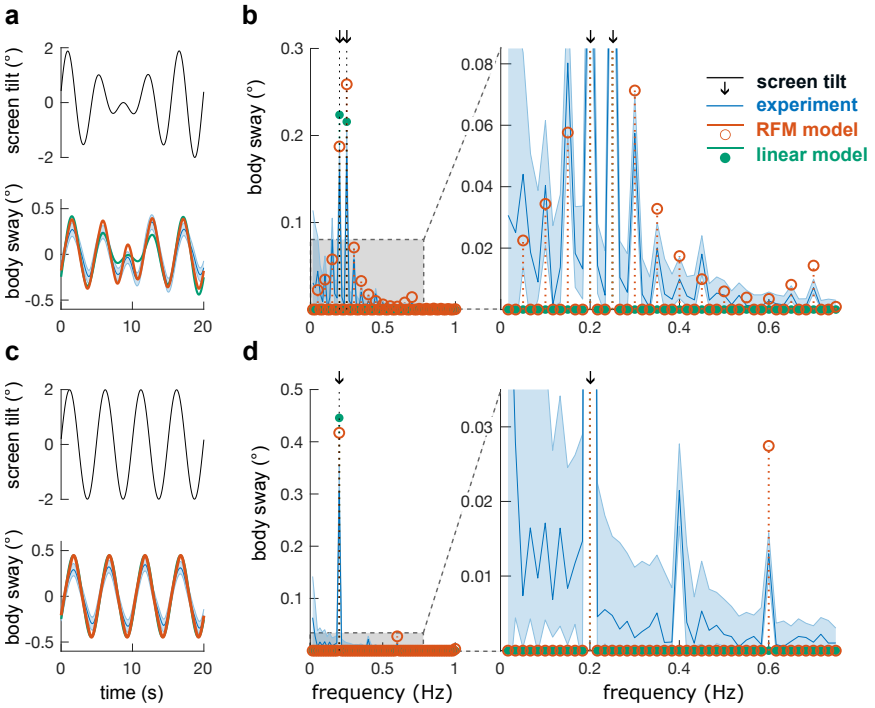

Figure 2: Model predictions and experimental results for sinusoidal visual scene movements. a) A waxing and waning stimulus (black) created by superimposing two sine waves with frequencies 0.2 and 0.25 Hz and sway responses predicted by the nonlinear model (orange) and the linear model with the RFM mechanism removed and the visual weight set to 4% to roughly match experimental sway response amplitudes (green). Experimental sway responses in the time domain averaged across 24 subjects and 18 repetitions of 20 s long sequences with 95% bootstrap confidence bounds (blue shade). b) Amplitude spectra of model predictions (orange circles) and of experimental sway responses (blue) with 95% bootstrap confidence bounds (Zoubir and Boashash, 1998). Spectra were calculated from 60 s data segments to increase the spectral frequency resolution, averaged across 6 repetitions per subject and 24 subjects. c) Time domain and d) amplitude spectra of experimental and model-predicted (orange)sway responses to a sinusoidal 0.2 Hz stimulus, using the same averaging as in a) and b), respectively. Linear model behavior is shown for comparison (green).

the Dokka et al. (2010) analysis). We found that the RFM model with our previously identified parameters (Figure 1d) displayed power-law behavior over a wide range of stimulus amplitudes thus demonstrating behavior that has been linked to Bayesian inference.

However, the response gains from the RFM model were systematically larger than the experimental data when using the parameters estimated for our subjects and conditions (Figure 1d). By lowering the model's visual weight, ω_{vis}, to 0.08 and 0.12 for the Mergner et al. (2005) data and the Peterka and Benolken (1995) data, respectively, good agreement was obtained to the experimental data (Figure 3). Notably, at very low stimulus velocities below about 0.2°/s the RFM gains were lower than expected from power-law behavior. Additional simulations exploring the model behavior with respect to parameter variation (not presented here) indicated that this deviation was strongly influenced by the dead-zone threshold λ.

3 Discussion

In the present study, we provide evidence that changes in sensory contributions to balance control emerge from a multisensory reconstruction of visual scene motion in the central nervous system. This mechanism is able to explain and predict less than proportional increases in sway response amplitudes with increasing stimulus amplitudes. The model further predicted spectral distortions with sway responses evoked at frequencies not present in the stimulus. Overall, the model was in excellent agreement, explaining and predicting experimental sway responses to a total of 7 stimuli with a VAF between 81% and 95%. In addition, the model is comparatively simple, with only 6 model parameters and a physiologically plausible architecture. Finally, we showed that the model reproduces power-law behavior across a wide

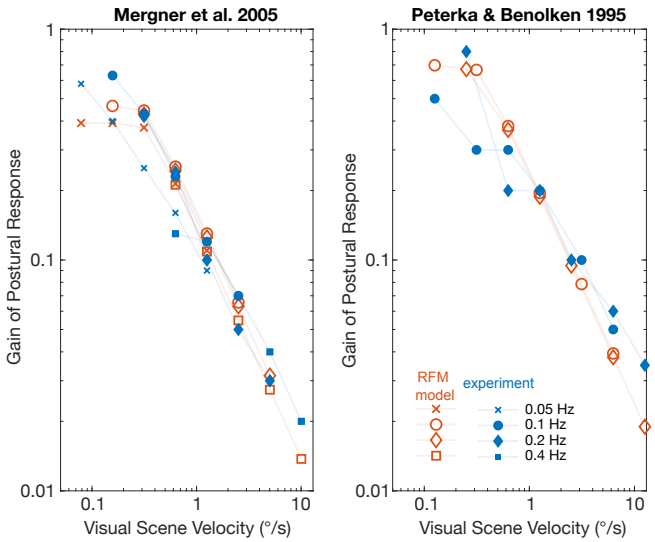

Figure 3: Model predictions and experimental results for sinusoidal visual scene movements across multiple amplitudes and frequencies. Experimental data was manually extracted from Figure 3 in Mergner et al. (2005) and Figure 4 in Peterka and Benolken (1995) and displayed as described in Dokka et al. (2010). RFM model results are for parameters as shown in Figure 1 with the exception of the visual weight, which was set to $\omega_{vis} = 0.08$ and $\omega_{vis} = 0.12$ for comparison with the Mergner et al. and Peterka and Benolken data, respectively.

range of stimulus velocities that has been related to sensory processing based on Bayesian inference principles (Dokka et al., 2010). In the following, we discuss the generality of RFM estimation and its potential role in noise reduction and causal inference.

Nonlinear RFM estimation may also play a role in other tasks that require an internal reconstruction of body orientation in space. In the current study, we used visual scene motion to induce sensory conflicts. However, the RFM estimator was inspired by models incorporating RFM-like mechanisms from previous studies. The models reproduced reweighting-like balance behavior induced by other RFMs, such as support surface tilts (Assländer et al., 2015; Mergner et al., 2003) or movements of a haptic reference (Assländer et al., 2018). The RFM concept is also consistent with human perception during sensory conflicts (Mergner et al., 1991). Mergner et al. (Mergner et al., 1991) found that humans perceive a slow rotation of the head relative to the body as a head rotation in space, even when the body is rotating underneath the fixed head. This illusion fades with increasing velocities and the body is increasingly correctly perceived as moving in space. This perceptual pattern was accounted for by a multisensory nonlinear RFM estimation, similar to the one presented here. The concept of RFM estimation is also consistent with the train illusion in which a train that begins to move is interpreted as self-motion rather than train motion. The self-motion illusion fades as the train speeds up and the RFM estimate starts to correct the visual input.

All of these results share a common framework. For the estimation of body orientation in space the CNS

1. calculates a multisensory RFM estimate,
2. uses the RFM estimate to correct a sensory input if it exceeds a certain velocity, and
3. integrates corrected sensory inputs with fixed weights.

The mechanism acts rapidly, thus meeting the requirements for MSI of continuous sensory signals in closed loop control tasks (Noel et al., 2023). Thus, the evidence from studies in balance control and perception indicate that nonlinear RFM estimation could be a general mechanism to resolve sensory conflicts in MSI.

Vestibular information likely plays a dominant role in RFM estimation. In our study, subjects stood on a fixed level surface. Thus, both proprioceptive and vestibular systems provided inputs from space-veridical reference frames. Assuming that both sensory inputs are used for the RFM estimation, we should see similar reweighting effects in subjects with normal sensory function and those with bilaterally absent vestibular function. However, previous studies showed that subjects without vestibular function were essentially unable to reweight visual information when standing on a fixed support surface (Peterka, 2002; Peterka and Benolken, 1995). Re-interpreting these results with respect to the

RFM mechanism, vestibular loss subjects seem to be unable to use proprioceptive cues for RFM estimations for visual scene movements. They appear to effectively use fixed sensory weights across all visual stimulus amplitudes. Thus, the gravito-inertial space reference provided by the vestibular system appears to be of primary importance for the RFM estimation.

One benefit of the RFM concept is the creation of context. For intelligent behavior, it is widely understood that the CNS utilizes an internal representation of the outside world. The RFM estimate constitutes such an internal representation of the external environment derived from the nonlinear processing of available sensory cues. Furthermore, intelligent behavior, in the sense of a context-dependent use of sensory information, emerges from this process. The underlying nonlinear processing of multi-sensory information infers changes in environmental conditions and generates rapid MSI changes that adjust for them. The RFM estimation as it applies to balance control can therefore be considered to represent the embodiment of a causal inference mechanism specifically designed to implement rapid compensation for a wide variety of balance disturbances.

Another major benefit of combining multiple sensory inputs is the reduction of variability and improvement of precision in estimates (Angelaki et al., 2009; Ernst and Banks, 2002; Faisal et al., 2008; Wolpert, 2007). This raises the question, whether the RFM estimator can have a noise reducing effect. An earlier study showed that a velocity dead-zone can reduce noise, by essentially blocking sub-threshold noisy signals (Mergner et al., 2009). The dead-zone in the RFM estimate could therefore achieve noise reduction by partly blocking noisy vestibular signals in situations of a stationary reference frame. The underlying assumption is that the vestibular system has a higher noise level than sensory signals from other reference frames. While it is inherently difficult to directly assess noise properties of a sensory system, there are studies that support this notion (van der Kooij and Peterka, 2011; Nouri and Karmali, 2018). The RFM concept would then represent a compromise between reducing noise and avoiding misinterpretations of sensory information when reference frames are moving and therefore unreliable. Such a trade-off between precision and accuracy is also captured by a Bayesian inference model, which has been used to explain the data presented in Figure 3 (Dokka et al., 2010). Unfortunately, a direct comparison of the RFM model and the proposed Bayesian model is not possible. Dokka et al. (2010) derived the power-law relation between gain values and stimulus velocity based on assumed noise properties in sensory systems using Bayesian statistics. Additionally, this derivation assumed an ideal transformation between sensed body motion and actual body motion. However, sensed body motion and actual body motion are dynamically linked through the closed-loop nature of the control system. The approach ignored these dynamic mechanisms needed to create corrective joint torques and achieve changes in body motion. Therefore, the Bayesian analysis differs considerably from control models, such as the RFM model, that do account for these dynamic properties of the balance control system. For example, gain and phase characteristics such as in Figure 1 e and f or frequency distortions such as in Figure 2 cannot be explained without accounting for the dynamic properties of the system. Implementing probabilistic considerations into feedback systems is a non-trivial task that needs to be addressed in future work.

We used a set of established simplifications to formulate our model. These include the concept of reference frames instead of individual peripheral sensory organ signals, the concept of body schema (i.e., 'visual' cues encode body orientation, rather than head orientation relative to the visual scene), modeling the body as a single inverted pendulum (neglecting coupling forces and potential hip and neck movements for head stabilization (De Nunzio et al., 2005)), assuming ideal transformations between position, velocity and acceleration signals, the assumption of a single lumped time delay, and noise-free sensory and central signals. The approach was tailored to experimentally assess and model the dynamics of MSI in a simplified system. Our goal was to uncover fundamental properties before adding complexity, which can make interpretations difficult if fundamental properties are not understood. For this purpose, we also constrained the range of stimulus amplitudes to avoid transient or voluntary movements, such as compensatory stepping caused by pushing subjects to their stability limits. Despite these simplifications, our model accounted for important features present in the experimental data.

One simplification stands out and likely affected our results. Sensory signals, neural processing and muscle contractions contain noise, leading to variability in body orientation estimates and resulting in random sway. This random sway component is superimposed on the sway evoked by the stimulus. Using a large amount of averaging, we reduced the random sway component in our experimental data and extracted the sway responses to the stimuli. In line with systems identification principles, we then reproduced and predicted these sway responses to the visual perturbation with our model. Thus, we did not explicitly include noise sources in our model. For linear systems, handling noise in this way is a valid approach (Pintelon and Schoukens, 2012) and has been widely used in MSI research. For nonlinear systems, the approach could result in systematic biases. A noteworthy interaction between noise and nonlinear dead-zone elements is stochastic resonance (Benzi et al., 1981). In the context of our model, the internal estimate $\dot{\varphi}_{screen}$ will fluctuate around the true value due to sensory noise. These fluctuations will occasionally cross the dead-zone threshold, even if $\dot{\varphi}_{screen}$ is, on average, below the threshold. Thus, sensory noise and stimulus characteristics likely interact unintuitively with the nonlinear dead-zone in the RFM mechanism. Explicitly accounting for internal noise sources could therefore further

improve model validity and predictions. Furthermore, these interactions could be used to identify noise properties at different locations in the feedback mechanism. Including stochastic components into a nonlinear feedback-control model requires mathematical methods tailored to the problem. Such tailored methods need to be developed in future work.

In conclusion, we present a simple sensory integration mechanism for balance control which reconstructs reference-frame motion in conditions where the visual scene is moving. We showed how a velocity dead-zone in the multisensory signal that combines visual motion information with space-referenced sensory signals leads to context-dependent changes of sensory contributions to balance. Additionally, this mechanism demonstrated a power-law stimulus-response relationship that has been related to Bayesian sensory integration principles. The mechanism can be considered to be a rapid-acting causal-inference mechanism suitable for use in a closed-loop feedback control system.

4 Methods

Subjects

Twenty-four subjects (23.3 ± 3.4 years; 172.7 ± 9.4 cm; 75.2 ± 10.9 kg) without any known balance disorders completed the study. Subjects gave written informed consent and were reimbursed with 20€ for participating in the study. The protocol was approved by the University of Konstanz IRB and was in agreement with the Declaration of Helsinki.

Experimental setup

Subjects stood upright wearing a Virtual Reality head-mounted display (HMD; Vive Pro Eye, HTC, Taoyuan, Taiwan) and had motion tracking markers (Vive Tracker, HTC, Taoyuan, Taiwan) attached between the shoulder blades and at greater trochanter height using Velcro straps. Subjects viewed a half-cylindrical screen (radius 1m) with high contrasting patterns (Figure 1). The screen was tilting in anterior-posterior direction, approximately around the ankle joint axes (8.8cm above the floor) following predefined waveforms. Marker positions were recorded with every display update at ≈90 Hz. Virtual environment and recording were implemented in a custom written software (Assländer et al., 2023) in Unity (Unity Technologies, San Francisco, USA) and SteamVR (Valve, Bellevue, USA). The software is freely available (https://github.com/PostureControlLab/anaropia-rfm/releases). Motion smoothing and automatic resolution were enabled in SteamVR to ensure a stable framerate during the whole experiment. Pseudorandom stimuli were constructed from 80-state ternary maximum-length sequences (Davies, 1970; Peterka, 2002). Four pseudorandom stimuli had 20-s duration cycles with 15 continuously repeated cycles and one stimulus had 10-s duration cycles with 30 repeated cycles (Figure 1e & f). Two different sine stimuli were used with durations of 380 s (Figure 2). The protocol included three stimuli not included in this manuscript. Following a 120 s long warmup test, with visual screen movements to familiarize subjects with the setup, the 10 stimulus conditions were presented in random order.

Data analysis

Raw data, scripts and model used for analysis are available at https://doi.org/10.17605/OSF.IO/EMSKV. We resampled the marker data to ensure a consistent 90 Hz sampling rate and calculated the whole-body center of mass sway using the subjects' height, weight and anthropometric tables (Assländer et al., 2023). The first 20 s of each trial was discarded to avoid transients and data was averaged across cycle repetitions and subjects. FRFs were calculated for pseudo-random stimuli by dividing average body sway spectra by the average stimulus spectra. Averages additionally included averaging across frequencies to obtain FRFs with approximately logarithmic frequency spacing (Peterka, 2002) For sine stimuli we averaged across the 432 single stimulus cycles to obtain across-subject time domain average responses (Figure 2, left column). Spectra were calculated from the average across 144 repetitions of 60-s duration data segments to obtain the desired spectral frequency resolution of 1/60 s = 0.017 Hz. For time domain and spectral data, we obtained 95% confidence bounds using 1000 bootstraps of the individual cycles and repeating the above described calculations. The 25th and 975th largest bootstrap values were used as upper and lower confidence bounds, respectively (Zoubir and Boashash, 1998).

Model simulations

The model was built in Simulink 2023b (The Mathworks, Natick, USA) using average subject anthropometrics to estimate moment of inertia and center of mass height. We fit model parameters to experimental frequency response functions H_e formulating the optimization problem as

$$\min_{\theta\ ,\beta} \sum_{j=0}^{M-1} \sum_{k=0}^{N-1} \log(2\beta\ |H_m(\theta,k,j)|)\ +\ \sum_{k=0}^{N-1} \frac{|H_e(k,j)\ -\ H_m(\theta,k,j)|}{\beta\ |H_m(\theta,k,j)|}$$

with the experimental and model FRFs H_e and H_m, the scale parameter of the Laplace distribution β, frequencies k, the three pseudorandom stimulus conditions j, and the parameter vector θ, containing the six model parameters P, D, K_{torque}, τ, λ, ω_{vis} (Assländer et al., 2023). We used a global optimization approach with the function 'GloabalSearch' ('Global Optimization Toolbox', Matlab 2023b, Mathworks, Natick, USA) and the algorithm 'fmincon'. Parameter bounds were set to physiologically plausible values and never reached during fitting procedures. To speed up the optimization process, we used an approximation of the dead-zone developed for this purpose. The RFM estimate entering the threshold is an internal reconstruction of the stimulus applied during the experiment. We therefore calculated transfer functions $H_{deadzone}(M,k,\lambda)$ dividing spectra of dead-zone input $\dot{\varphi}_{screen}$ and output $\dot{\varphi}_{out}$ calculated from

$$\begin{aligned} \dot{\varphi}_{screen} - \lambda, \text{ for } \dot{\varphi}_{screen} > \lambda \\ \dot{\varphi}_{out}\ =\ 0, \text{ for } |\dot{\varphi}_{screen}| \leq \lambda \\ \dot{\varphi}_{screen} + \lambda, \text{ for } \dot{\varphi}_{screen} < \lambda \end{aligned}$$

$H_{deadzone}(M,k,\lambda)$ was calculated for λ from 0 to 1°/s in steps of 0.01°/s. For intermediate λ values, we calculated the weighted average of adjacent λ entries in the $H_{deadzone}(M,k,\lambda)$ table. Then the model shown in Figure 1 can be formulated in the frequency domain using

$$H_m(\theta,k,j) = \frac{\omega_{vis}(1 - H_{deadzone})B\ C}{1 - T\ C\ +\ B\ C}$$

with the body dynamics $B = \frac{1}{Js^2 - mgh}$ with the Laplace variable s inertia J, body mass m, center of mass height h and the gravitational constant g, motor activation including time delay $C = (P + Ds)\ \exp^{-s\ \tau}$, and the positive torque feedback $T = \frac{K_{torque}}{s}$. We compared the formulation of H_m to Simulink model formulations to confirm their equivalence.

Following the parameter fits to the FRFs of the first three pseudorandom data sets (Figure 1e), model simulations for all five pseudorandom stimuli were run in Simulink. Then time domain and frequency domain model outputs were calculated analogous to the analysis of experimental data. Linear model simulations were performed using the same procedure and the same model, fully blocking the RFM estimator path to obtain a MSI mechanism consisting of a linear weighted sum.

References

D. E. Angelaki, Y. Gu, and G. C. DeAngelis. Multisensory integration: psychophysics, neurophysiology, and computation. *Current Opinion in Neurobiology*, 19(4):452–458, 2009. ISSN 09594388. doi:10.1016/j.conb.2009.06.008.

L. Assländer, G. Hettich, and T. Mergner. Visual contribution to human standing balance during support surface tilts. *Human Movement Science*, 41:147–164, 2015. doi:10.1016/j.humov.2015.02.010. URL `http://linkinghub.elsevier.com/retrieve/pii/S016794571500038X`.

L. Assländer, C. P. Smith, and R. F. Reynolds. Sensory integration of a light touch reference in human standing balance. *PloS one*, 13(6):e0197316–e0197316, 2018. doi:10.1371/journal.pone.0197316.

L. Assländer, M. Albrecht, M. Diehl, K. J. Missen, M. G. Carpenter, and S. Streuber. Estimation of the visual contribution to standing balance using virtual reality. *Scientific Reports*, 13(1):2594, 2023. ISSN 2045-2322. doi:10.1038/s41598-023-29713-7. URL `https://www.nature.com/articles/s41598-023-29713-7`.

R. Benzi, A. Sutera, and A. Vulpiani. The mechanism of stochastic resonance. *Journal of Physics A: mathematical and general*, 14(11):L453, 1981.

S. Carver, T. Kiemel, and J. J. Jeka. Modeling the dynamics of sensory reweighting. *Biological cybernetics*, 95(2): 123–134, 2006.

K. E. Cullen. Vestibular processing during natural self-motion: implications for perception and action. *Nature Reviews Neuroscience*, 20(6):346–363, 2019. ISSN 14710048. doi:10.1038/s41583-019-0153-1. URL `http://dx.doi.org/10.1038/s41583-019-0153-1`. Publisher: Springer US.

W. Davies. *System Identification for Self-Adaptive Control*. Wiley-Interscience, 1970.

A. M. De Nunzio, A. Nardone, and M. Schieppati. Head stabilization on a continuously oscillating platform: The effect of a proprioceptive disturbance on the balancing strategy. *Experimental Brain Research*, 165(2):261–272, 2005. ISSN 00144819. doi:10.1007/s00221-005-2297-7. ISBN: 0014-4819 (Print)\n0014-4819 (Linking).

K. Dokka, R. V. Kenyon, E. a. Keshner, and K. P. Kording. Self versus environment motion in postural control. *PLoS computational biology*, 6(2):e1000680–e1000680, 2010. doi:10.1371/journal.pcbi.1000680. URL `http://www.pubmedcentral.nih.gov/articlerender.fcgi?artid=2824754&tool=pmcentrez&rendertype=abstract`.

M. O. Ernst and M. S. Banks. Humans integrate visual and haptic information in a statistically optimal fashion. *Nature*, 415(6870):429–433, 2002.

A. A. Faisal, L. P. J. Selen, and D. M. Wolpert. Noise in the nervous system. *Nature Reviews Neuroscience*, 9:292–303, 2008. ISSN 1471-0048 (Electronic)\r1471-003X (Linking). doi:10.1038/nrn2258.

C. R. Fetsch, A. H. Turner, G. C. DeAngelis, and D. E. Angelaki. Dynamic reweighting of visual and vestibular cues during self-motion perception. *The Journal of Neuroscience*, 29(49):15601–15612, 2009. ISSN 0270-6474, 1529-2401. doi:10.1523/JNEUROSCI.2574-09.2009. URL `https://www.jneurosci.org/lookup/doi/10.1523/JNEUROSCI.2574-09.2009`.

C. R. Fetsch, A. Pouget, G. C. Deangelis, and D. E. Angelaki. Neural correlates of reliability-based cue weighting during multisensory integration. *Nature Neuroscience*, 15(1):146–154, 2012. ISSN 10976256. doi:10.1038/nn.2983.

F. Horak and J. Macpherson. Postural orientation and equilibrium. In S. R. Geiger, editor, *Handbook of Physiology - Section 12*, pages 255–292. American Physiological Soc., 1996. ISBN 0-19-509174-4.

H. Imamizu, S. Miyauchi, T. Tamada, Y. Sasaki, R. Takino, B. PuÈtz, T. Yoshioka, and M. Kawato. Human cerebellar activity reflecting an acquired internal model of a new tool. *Nature*, 403(6766):192–195, 2000.

T. Kiemel, A. J. Elahi, and J. J. Jeka. Identification of the plant for upright stance in humans: multiple movement patterns from a single neural strategy. *Journal of neurophysiology*, 100(6):3394–3406, 2008.

K. P. Körding, U. Beierholm, W. J. Ma, S. Quartz, J. B. Tenenbaum, and L. Shams. Causal inference in multisensory perception. *PLoS ONE*, 2(9), 2007. ISSN 19326203. doi:10.1371/journal.pone.0000943.

R. Laboissière, J.-C. Letievant, E. Ionescu, P.-A. Barraud, M. Mazzuca, and C. Cian. Relationship between spectral characteristics of spontaneous postural sway and motion sickness susceptibility. *PLOS ONE*, 10(12):e0144466, 2015. ISSN 1932-6203. doi:10.1371/journal.pone.0144466. URL `https://journals.plos.org/plosone/article?id=10.1371/journal.pone.0144466`. Publisher: Public Library of Science.

J. Laurens and D. E. Angelaki. A unified internal model theory to resolve the paradox of active versus passive self-motion sensation. *eLife*, 6:e28074, 2017. ISSN 2050-084X. doi:10.7554/eLife.28074. URL `https://doi.org/10.7554/eLife.28074`. Publisher: eLife Sciences Publications, Ltd.

D. N. Lee and J. R. Lishman. Visual proprioceptive control of stance. *Journal of Human Movement Studies*, 1:87–95, 1975. URL `http://psycnet.apa.org/psycinfo/1976-27111-001`. Publisher: Teviot Scientific Publications.

T. Mergner, C. Siebold, G. Schweigart, and W. Becker. Human perception of horizontal trunk and head rotation in space during vestibular and neck stimulation. *Experimental brain research*, 85(2):389–404, 1991. ISSN 0014-4819. doi:10.1007/BF00229416. URL `http://www.ncbi.nlm.nih.gov/pubmed/1893987`. ISBN: 0014-4819 (Print)\n0014-4819 (Linking).

T. Mergner, C. Maurer, and R. J. Peterka. A multisensory posture control model of human upright stance. *Progress in brain research*, 142(1):189–201, 2003. doi:10.1016/S0079-6123(03)42014-1. URL `http://www.ncbi.nlm.nih.gov/pubmed/12693262`.

T. Mergner, G. Schweigart, C. Maurer, and A. Blümle. Human postural responses to motion of real and virtual visual environments under different support base conditions. *Experimental brain research*, 167:535–556, 2005.

T. Mergner, G. Schweigart, L. Fennell, and C. Maurer. Posture control in vestibular-loss patients. *Annals of the New York Academy of Sciences*, 1164:206–15, 2009. ISSN 1749-6632. doi:10.1111/j.1749-6632.2008.03722.x. URL `http://www.ncbi.nlm.nih.gov/pubmed/19645901`.

K. J. Missen, L. Assländer, A. Babichuk, R. Chua, J. T. Inglis, and M. G. Carpenter. The role of torque feedback in standing balance. *Journal of Neurophysiology*, 130(3):585–595, 2023. ISSN 1522-1598. doi:10.1152/jn.00046.2023.

M. L. Morgan, G. C. DeAngelis, and D. E. Angelaki. Multisensory integration in macaque visual cortex depends on cue reliability. *Neuron*, 59(4):662–673, 2008. ISSN 08966273. doi:10.1016/j.neuron.2008.06.024. URL `https://linkinghub.elsevier.com/retrieve/pii/S0896627308005679`.

L. Nashner and A. Berthoz. Visual contribution to rapid motor responses during postural control. *Brain research*, 150 (2):403–7, 1978. ISSN 0006-8993. URL http://www.ncbi.nlm.nih.gov/pubmed/678978.

J.-P. Noel and D. E. Angelaki. Cognitive, systems, and computational neurosciences of the self in motion. *Annual review of psychology*, 73:103–129, 2022. ISSN 1545-2085. doi:10.1146/annurev-psych-021021-103038. URL http://www.ncbi.nlm.nih.gov/pubmed/34546803.

J. P. Noel, J. Bill, H. Ding, J. Vastola, G. C. Deangelis, D. E. Angelaki, and J. Drugowitsch. Causal inference during closed-loop navigation: Parsing of self- and object-motion. *Philosophical Transactions of the Royal Society B: Biological Sciences*, 378(1886), 2023. ISSN 14712970. doi:10.1098/rstb.2022.0344. Publisher: Royal Society Publishing.

S. Nouri and F. Karmali. Variability in the vestibulo-ocular reflex and vestibular perception. *Neuroscience*, 393:350–365, 2018. ISSN 03064522. doi:10.1016/j.neuroscience.2018.08.025. URL https://linkinghub.elsevier.com/retrieve/pii/S0306452218305700.

T. Ohshiro, D. E. Angelaki, and G. C. Deangelis. A normalization model of multisensory integration. *Nature Neuroscience*, 14(6):775–782, 2011. ISSN 10976256. doi:10.1038/nn.2815.

J. H. Pasma, D. Engelhart, A. B. Maier, A. C. Schouten, H. van der Kooij, and C. G. M. Meskers. Changes in sensory reweighting of proprioceptive information during standing balance with age and disease. *Journal of neurophysiology*, 114(6):3220–33, 2015. doi:10.1152/jn.00414.2015. URL http://www.ncbi.nlm.nih.gov/pubmed/26424578.

R. J. Peterka. Sensorimotor integration in human postural control. *Journal of neurophysiology*, 88(3):1097–118, 2002. ISSN 0022-3077. URL http://www.ncbi.nlm.nih.gov/pubmed/13679407.

R. J. Peterka and M. S. Benolken. Role of somatosensory and vestibular cues in attenuating visually induced human postural sway. *Experimental brain research*, 105(1):101–110, 1995. URL http://www.ncbi.nlm.nih.gov/pubmed/7589307.

R. Pintelon and J. Schoukens. *System Identification: A Frequency Domain Approach*. John Wiley & Sons, 2012. ISBN 0470640375. Pages: 743.

B. Riecke, B. Murovec, J. Campos, and B. Keshavarz. Beyond the eye: Multisensory contributions to the sensation of illusory self-motion (vection). *Multisensory Research*, 36:1–38, 2023. doi:10.1163/22134808-bja10112.

H. van der Kooij and R. J. Peterka. Non-linear stimulus-response behavior of the human stance control system is predicted by optimization of a system with sensory and motor noise. *Journal of computational neuroscience*, 30(3): 759–78, 2011. ISSN 1573-6873. doi:10.1007/s10827-010-0291-y. URL http://www.pubmedcentral.nih.gov/articlerender.fcgi?artid=3108015&tool=pmcentrez&rendertype=abstract. ISBN: 1573-6873 (Electronic)\n0929-5313 (Linking).

H. van der Kooij, R. Jacobs, B. Koopman, and F. van der Helm. An adaptive model of sensory integration in a dynamic environment applied to human stance control. *Biological cybernetics*, 84(2):103–15, 2001. ISSN 0340-1200. URL http://www.ncbi.nlm.nih.gov/pubmed/11205347.

D. M. Wolpert. Probabilistic models in human sensorimotor control. *Human movement science*, 26(4):511–524, 2007. ISSN 0167-9457. doi:10.1016/j.humov.2007.05.005. URL http://www.pubmedcentral.nih.gov/articlerender.fcgi?artid=2637437&tool=pmcentrez&rendertype=abstract.

D. M. Wolpert, Z. Ghahramani, and M. I. Jordan. An internal model for sensorimotor integration. *Science*, 269(5232): 1880–1882, 1995. ISSN 0036-8075, 1095-9203. doi:10.1126/science.7569931. URL https://www.science.org/doi/10.1126/science.7569931.

A. Zoubir and B. Boashash. The bootstrap and its application in signal processing. *IEEE Signal Processing Magazine*, 15(1):56–76, 1998. ISSN 10535888. doi:10.1109/79.647043. URL http://ieeexplore.ieee.org/lpdocs/epic03/wrapper.htm?arnumber=647043.